Salivary glands

Th. Vogl

T. J. Vogl, W. Reith, E. J. Rummeny (Eds.), *Diagnostic and Interventional Radiology*,
DOI 10.1007/978-3-662-44037-7_16,

16.1 Normal Topography, Special Investigation Techniques and Specific Imaging Findings

16.1.1 Normal Topography

Parotid Gland

The parotid gland is the largest salivary gland in the **parotid area**; in addition, it involves the facial nerve, the retromandibular vein, the branches of the external carotid artery and the intraparotid lymph nodes. It is important to understand the course of the facial nerve that emerges from the mastoid foramen of the skull base, reaching the dorsal gland and dividing into five branches. It divides the parotid gland into a deep lobe and a superficial lobe. Diagnosis must be based on the course of each of the excretory ducts of the parotid gland.

Submandibular Gland

The submandibular gland is the second largest salivary gland, and opens through the Wharton's duct sublingual along the floor of the mouth in the caruncle. In the box of the submandibular in addition to the anterior belly of the digastrics muscle, the hypoglossal nerve and adipose tissue gland can be found. The submandibular gland lies under the mucous membrane on the ventral floor of the mouth on the mylohyoid muscle. In the compartment of the sublingual gland runs the lingual nerve as well as the branches of the glossopharyngeal and hypoglossal nerve.

16.1.2 Special Investigation Techniques

In the region of the salivary glands three major paired glands, the parotid, submandibular, sublingual and several hundred small salivary glands throughout the pharynx and the parapharyngeal space, are located.

The most common **clinical symptoms** are unilateral or bilateral swelling of the affected gland. The swelling may be associated with pain or without symptoms. Other symptoms may occur as hyper-/hyposalivation or a sialorrhoea/Sicca syndrome.

The pathogenesis is usually neoplastic lesions, obstructive/inflammatory changes or glandular involvement as part of a systemic disease. Clinically, in addition to the medical history should examine by palpation and laboratory studies.

Diagnostic imaging includes the use of sonography as the first diagnostic tool, further supplemented by CT, MRI, and in some cases, the sialography.

Conventional Radiography

For conventional radiography specific investigation techniques include the postero-anterior and craniocaudal projection, as well as oblique, usually for the detection of gallstones, but they must be at least 2–3 mm in size (Fig. 16.1).

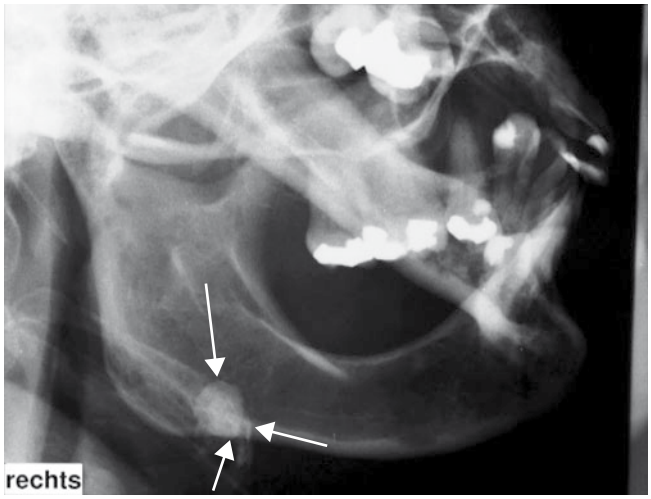

Fig. 16.1 Calculus of the submandibular gland. On the radiograph the oblique lateral view of a well-circumscribed homogeneous increased projection zone in the mandible (*arrows*). This finding corresponds to a calculus in the submandibular gland

Sialography

Through the application of a water-soluble iodinated contrast agent into the excretory duct of the parotid gland or the submandibular salivary gland a contrast of the salivary glands and its ramifications. Ectasia, stenosis and response terminations are evaluated in the context of inflammatory or neoplastic processes.

The risks of the procedure lie in the extravasation of contrast medium in infection and abscess formation. Therefore, sialography is contraindicated in the inflammatory phase and is increasingly being replaced by MR sialography.

Sonography

Sonography is usually the first-line imaging technique, using a 7.5-MHz transducer. Using these techniques intra- and extra glandular lesions are differentiated and an attempt is made to differentiate benign from malignant lesions. The deep lobe of the parotid gland and lesions in the mandibular angle and in the parapharyngeal/retropharyngeal space are usually not represented.

CT

The computed tomographic diagnosis of the salivary gland is part of an evaluation of the facial skull and neck region. In general, this is now performed on multislice computed tomography, after application of contrast medium (100–150 ml). The evaluation is based on axial, coronal to sagittal MPR reconstructions.

Magnetic Resonance Imaging

Magnetic resonance imaging is the primary imaging modality for the diagnosis of salivary glands, i.e. the diagnosis of lesions and opaque processes of the salivary glands.

This is done usually with strongly T1- and T2-weighted spin-echo sequences in axial and coronal planes, supported by

Fig. 16.2 Normal topography of the major salivary glands (parotid gland on both sides). T1-weighted fat-suppressed spin-echo sequence, TR/TE = 500 / 22, gadolinium DTPA. Documentation of the superficial (*arrows*) and deep (*arrowheads*) lobes of the parotid gland on both sides. Increased signal intensity in comparison to the fatty tissue of the parotid gland. Exemplary of the usually sharp spur of the glandular tissue

fat-suppressed sequences and after administration of contrast medium (Fig. 16.2). Overall, sequences with high spatial resolution (matrix 256 × 512) should be carried out.

The MR sialography can be done using heavily T2-weighted sequences, e.g. by means of sequences such as RARE ("rapid acquisition with relaxation enhancement") and 3-DCISS ("constructive interference in steady state"). The use of STIR sequences complements the diagnostic information.

16.1.3 Specific Imaging Findings

The diagnosis of salivary glands by sonography, CT and MRI is based on the analysis of the following **diagnostic criteria**:

- Intra- and extra-glandular process
- Type of tumour growth
- Assessment of the edge structure
- Topographic spread of the neoplastic process
- Infiltration of the skull base
- Staging of lymph nodes

The image analysis involves the detection of calcifications (usually on CT) to differentiate a stone disease (Fig. 16.1) or a stone conglomerate. Cystic lesion of the parotid gland, the parotid and sublingual gland are thus differentiated (Overviews).

Cystic Lesions of the Parotid Gland

- Variations: branchial arch
- Inflammatory changes:
  - Abscess
  - Lymph node metastasis
  - Obstruction of the salivary duct
  - Lymphoepithelial cysts (HIV infection)
- Tumours:
  - Cystadenolymphoma, Warthin's tumour
  - Cystic schwannoma, neurofibroma
  - Pleomorphic adenoma
  - Mucoepidermoid carcinoma
  - Cystic hygroma

Cystic Lesions of the Submandibular and Sublingual Glands

- Variations: branchial cyst, second arch
- Inflammatory changes:
  - Abscess
  - Mucocele
  - Obstruction
- Tumourous changes:
  - Dermoid cyst
  - Cystic hygroma
  - Colloid cysts
  - Epidermoid
  - Lipomas

General Differential Diagnosis of Lesions of the Submandibular and Sublingual Glands

- **Congenital changes:**
  - Branchial cyst
  - Cystic hygroma
  - Dermoid
- Inflammatory changes:
  - Lymphadenopathy
  - Sialoadenitis
  - Ranula
  - Phlegmon
  - Abscess
- **Tumours:**
  - Benign:
    - Lipoma
    - Epidermoid
    - Pleomorphic adenoma
  - Malignant:
    - Mucoepidermoid carcinoma
    - Adenocystic carcinoma
    - Lymphoma
    - Infiltration of secondary metastases

- **Other space-occupying lesions:**
  - Sjögren's disease
  - Pseudotumour
  - Lymph node

16.2 Malformations/Abnormalities

No diagnostically relevant issues.

16.3 Trauma Issues

No diagnostically relevant issues

16.4 Inflammatory Issues

Sialoadenitis

As a rule there is no indication for diagnostic imaging in inflammatory changes. Only in the case of complications, it may be necessary.

Sialography is contraindicated in the acute phase. CT is used to detect calcification.

In order to detect abscesses/cellulitis changes a contrast-enhanced CT should be carried out (Fig. 16.3).

The particular value of MRI lies in the detection of inflammatory changes in patients with sialoadenitis (Fig. 16.4), such as Sjögren's disease (Fig. 16.5). The MRI shows accumulations of fluid (saliva within the gland). This can also be detected by MR sialography. Chronic sialoadenitis/adenosis results in shrinkage of the gland, and later, intraglandular calcifications. This leads then to the typical example of a leafless tree on MR sialography.

Ranula

The sublingual ranula manifests clinically as a painless swelling of the parotid. These scans are a result of post-inflammatory retention cysts with a surrounding epithelium. On imaging a ranula cannot be differentiated from a cystic hygroma or epidermoid. In complicated cases of ranula the signal textures are different.

16.5 Tumours

The one-sided, non-painful swelling of the affected salivary gland is the leading clinical symptom of a tumourous mass.

Rule of thumb: the smaller the affected gland is, the higher the probability of a malignant process. 50–81% of neoplastic lesions of the sublingual gland are malignant, as opposed to only about 20–25% of tumours of the parotid gland.

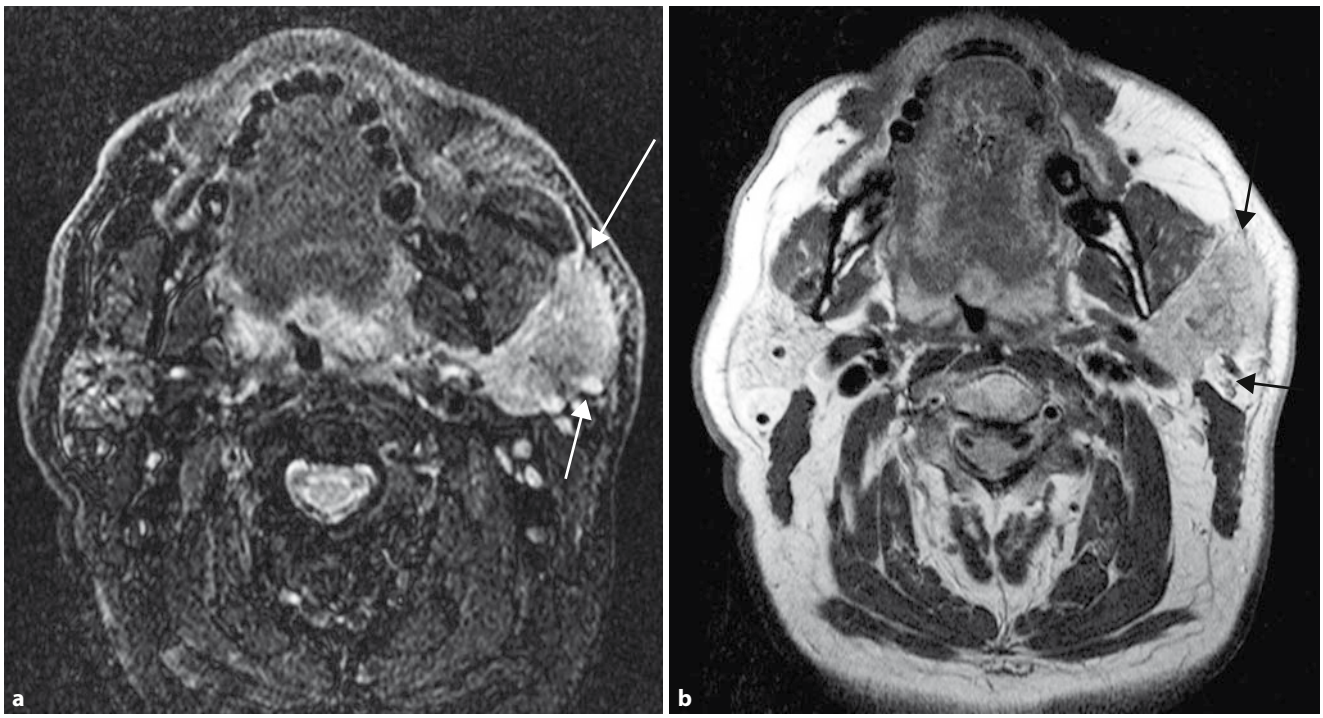

Fig. 16.3a,b Acute bacterial parotitis left side, MRI. a T2-weighted fat suppression spin-echo sequence. Mass on the left side of the parotid gland, affecting the organ diffusely (*arrows*), superficial and deep lobes. Confluent increased signal texture. No area of infiltration. Exemplary signal intensity the parotid gland on the right side. **b** On the T1-weighted sequence diffuse swelling in the parotid gland on the left side (*arrows*), blurred demarcation of the oedema of the masseter muscle. On the left side, there is no necrosis

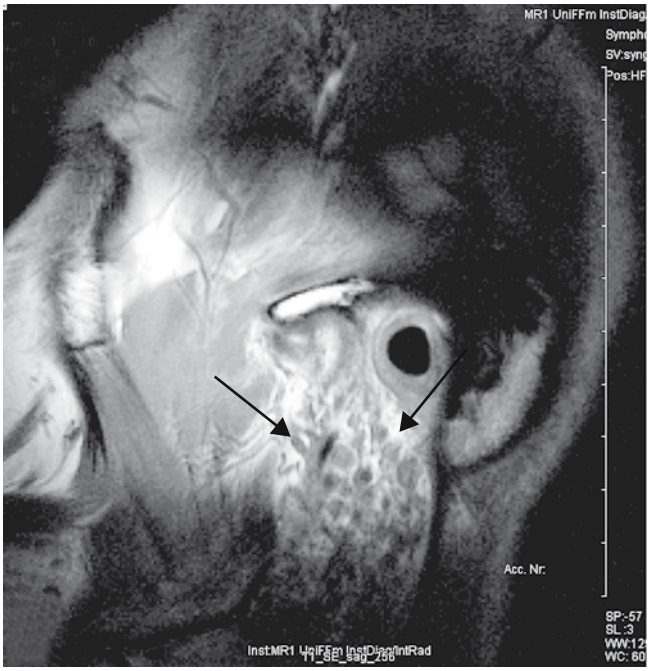

Fig. 16.4 Sialoadenitis. Sagittal T1-weighted sequence with an unenhanced parotid gland and presentation of the temporomandibular joint. T1-weighted SE sequence, TR/TE = 500 / 17. On the T1-weighted sequence documentation of a salt and pepper pattern of the parotid gland (*arrow*) with hypointense cystic internal structures. Hyperintense: chronic inflammatory changes in the parenchymal gland

Magnetic resonance imaging is the superior imaging modality. This is the characterisation of tumours by the analysis of T1- and T2-weighted sequences, and the documentation of contrast agent enhancement and the acquisition of infiltrative growth. Special attention needs to be drawn to perineural tumour spread evaluation directed towards the skull base, especially in adenoid cystic carcinoma.

Perineural tumour spread can occur along the stylomastoid foramen (facial nerve), the foramen oval (trigeminal, three branches), the foramen rotundum (trigeminal, two branches) and is visible after administration of contrast medium with strong enhancement.

The diagnostic scanning differentiation of benign and malignant lesions is often limited. With cystic lesions in particular, the distinction has become difficult. The pleomorphic adenoma usually shows strong enhancement of the entire tumour, but there may also be some necrosis.

Clinically, **benign tumours** of the salivary glands have the following characteristics:

- Slow growth for months or years
- Elastic rebound, freely movable nodes

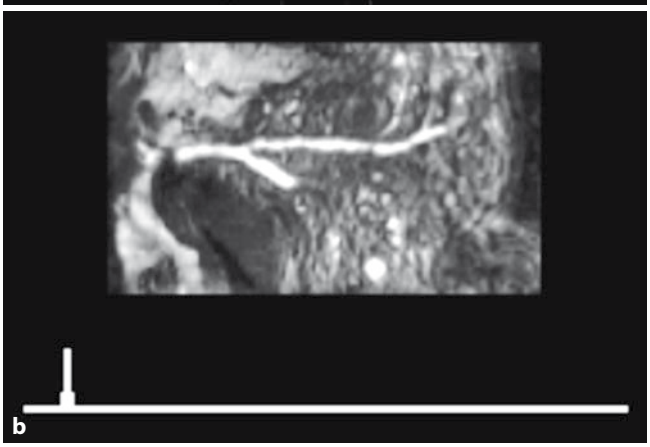

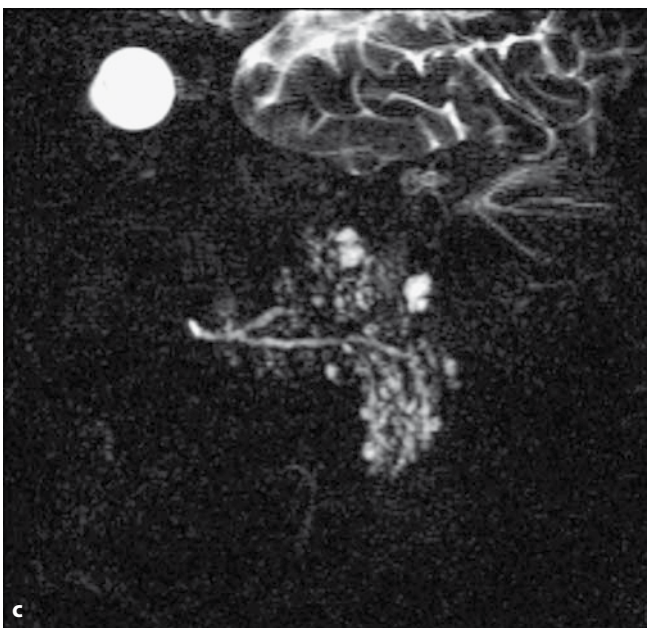

Fig. 16.5a–c Sjögren's disease, lymphoepithelial cysts. a T2-weighted axial spin-echo sequence, TR/TE = 3,090 Swelling of the parotid gland on both sides. Multiple signal increases smooth margins (*arrows*), cystic nature, in the parotid gland on both sides in terms of lymphoepithelial cysts in the underlying Sjögren's disease. **b, c** MR sialography: heavily T2-weighted sequence. Documentation of multiple hyperintense foci in the terms of the cysts

- No desmoplastic reaction
- No pathological lymphadenopathy

Malignant tumours, on the other hand, show:
- Rapid growth
- Lack of movability
- Often environmental infiltration

Haemangioma

In the paediatric patient population haemangioma is often found as a benign tumour. Haemangiomas are present in 61% at birth and are diagnosed in 84% within the 1st month of life.

Imaging. Imaging characteristics are strong enhancement after I.V. contrast agent administration and increased signal intensity on T2-weighted sequences. Diagnostic criteria are:
- Strong enhancement
- High signal intensity on T2-weighted sequences
- Blood flow-induced signal loss (flow voids on T1 and T2 sequences)
- Strong enhancement after administration of gadolinium DTPA

In children, cystic hygroma and lymphangiomas are also often diagnosed. Here, the cystic nature is apparent, especially on the MRI sequences.

Pleomorphic Adenoma

The most common benign tumour (Fig. 16.6) is the pleomorphic adenoma. Clinically, there is a progressive increase in the size of the affected salivary gland and a well-circumscribed, solid, solitary, easily palpable mass. Malignant degeneration is a complication of an untreated tumour.

Imaging. On CT pleomorphic adenoma appears hypodense, with rounded borders and clearly delineated from the surrounding parenchyma, with enhancement after contrast agent administration. With its increasing size, the tumour appeared heterogeneous and in hypodense areas, sometimes with calcifications. Magnetic resonance signal to an intermediate behaviour is found on the T1-weighted images and high signal on T2-weighted images as well as a strong analogy to CT contrast agent enhancement. Bleeding into the T1-weighted sequences complicates the differential diagnosis of malignancy.

Cystadenolymphoma/Warthin's Tumour

The second most common tumour of the parotid gland is Warthin's-tumour (Fig. 16.7), which originates from lymphatic tissue.

Imaging. The cystic appearance was apparent. On MRI, therefore, similar signal behaviour results with often constant marginal contrast enhancement.

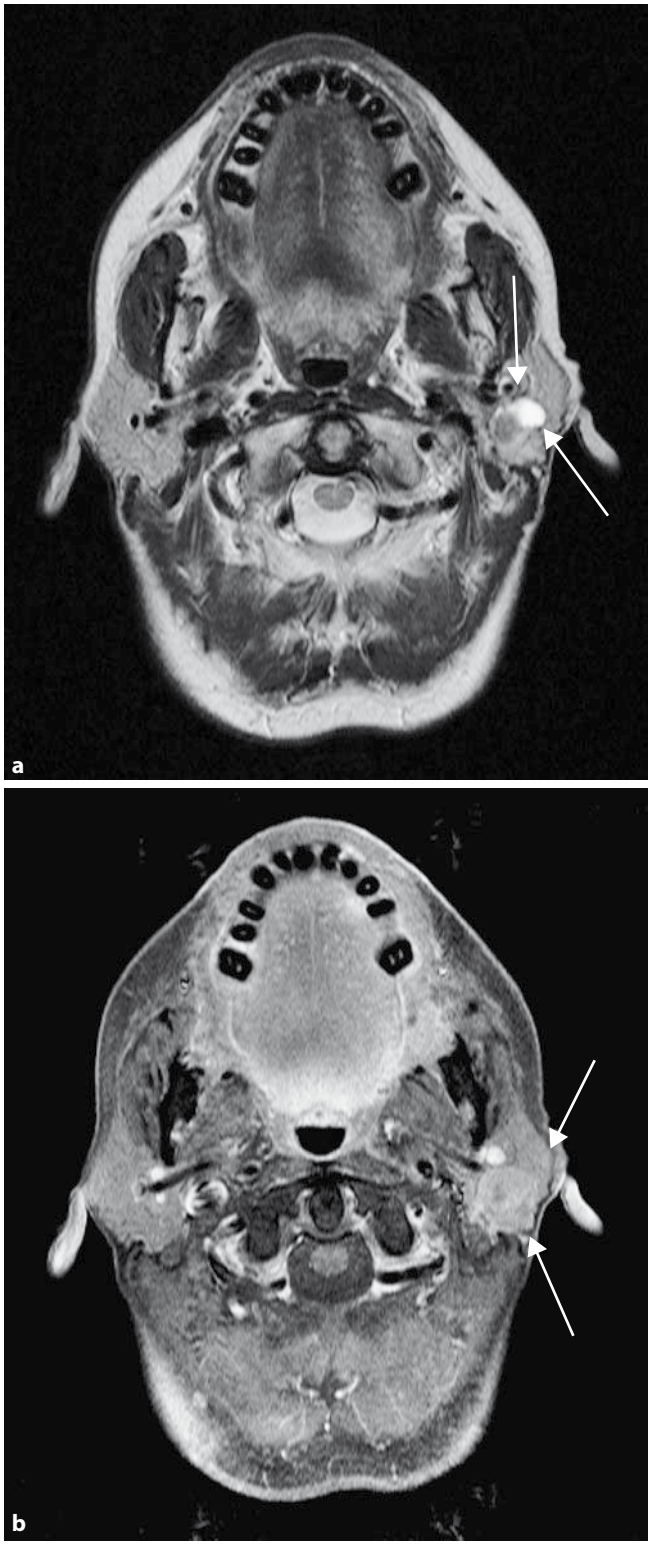

Fig. 16.6a,b Benign tumours: pleomorphic adenoma of the left parotid gland. a Proton density-weighted sequence, TR/TE = 3,000 / 25. On the proton density-weighted sequence rule-like anatomy and morphology of the normal parotid gland on the right side. Left side shows a mass lesion in the posterior parotid overlapping with a moderately increased signal intensity in the central intraparotid area of increased signal intensity, diameter 5 × 5 mm. **b** Fat suppressed T1-weighted spin-echo sequence, TR/TE = 500 / 17, gadolinium DTPA. Increased vascularity in the mass in the posterior parotid overlap; size and morphology speak in favour of the existence of a pleomorphic adenoma

Lipoma

The lipoma is found both within the parotid gland (Fig. 16.8) and in the surrounding area.

Imaging. Low density on CT and high signal on T1- and T2-weighted spin-echo sequences are typical, usually without capsule formation.

Tumours of Neural Origin

These tumours usually arise from the facial nerve and are often associated with neurofibromatosis type I. The morphology often shows on MRI as a heterogeneous appearing tumour.

Malignant Tumours

In the differentiation of malignant tumours of the salivary glands in essence the adenocarcinoma is differentiated (Fig. 16.9). The cancer may come from the large salivary glands, parotid, submandibular and sublingual glands.

The regional lymph nodes seem to be the cervical lymph nodes. With regard to the TNM classification one of the following applies:

- Tumour stage T1, when a tumour is < 2 cm, without extraparenchymal propagation.
- Tumour stage T2, if the tumour is > 2 cm but < 4 cm.
- Tumour stage T3, measuring > 4 cm
- Tumour stage T4a: tumour infiltration of skin, lower jaw and external auditory canal
- Tumour stage T4b: tumour invades the skull base, pterygoid process and surrounds the internal carotid artery

The classification of the lymph nodes corresponds to that of the other head and neck cancers.

Imaging. Tumours usually appear with massive contrast uptake. The soft-tissue infiltration can be documented precisely. **Magnetic resonance imaging** has been proven to be the optimal imaging modality for the differentiation of intra- and extraparotid portions of the tumour and for the detection of infiltration characteristics in the area of the skull base and neighbouring structures This should be carried out using T2- and T1-weighted sequences and involve diffusion-weighted sequences in order to obtain clarification.

Rare malignant tumours of the major salivary glands such as lymphoma, a rare neuroendocrine carcinoma or rarely squamous cell carcinomas must be differentiated. The lymphoma usually appears as a homogeneous mass with moderately elevated signal intensity on T2-weighted sequences, and the excessive loss of signal on T1-weighted sequences.

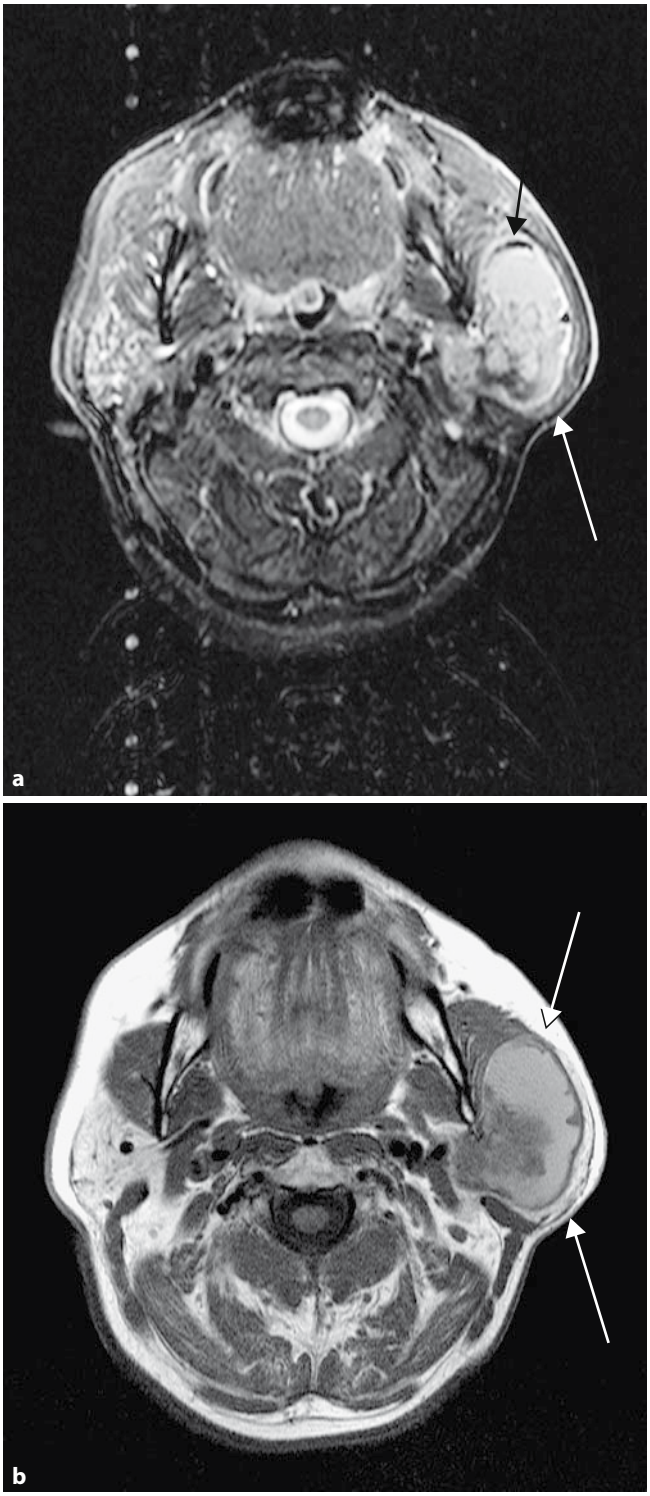

Fig. 16.7a,b Warthin's tumour (cystadenolymphopathy). a T2-weighted spin-echo sequence, TR/TE = 3,000 / 19. Swelling of the parotid gland on the left side, such a deeply superficial lobe with medial necrosis (*arrows*). **b** T1-weighted spin echo sequence, TR/TE = 500 / 22. Mass engaging the entire parotid gland. Peripheral edge with increased signal pattern. The liquid central zones show significant signal loss

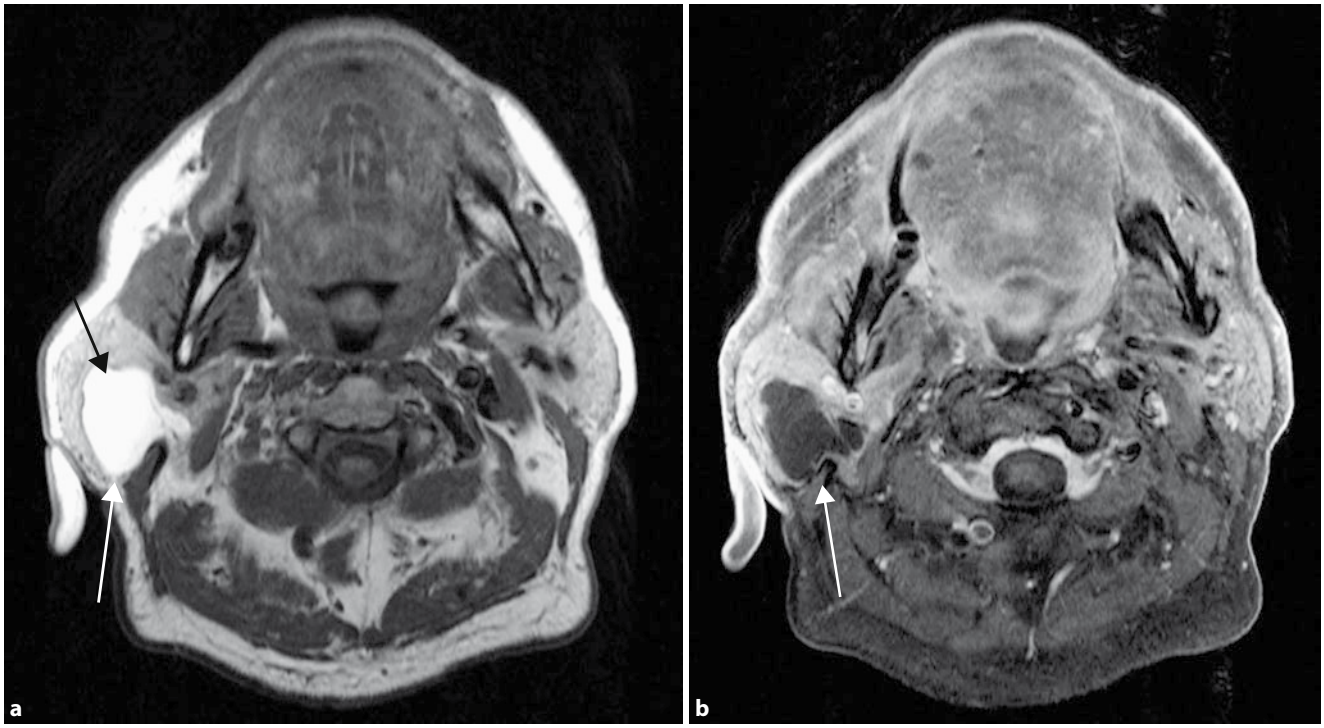

Fig. 16.8a,b Lipoma of the parotid gland on the right side. a T1-weighted spin-echo sequence, TR/TE = 500 / 17, unenhanced. High signal intensity of the lesion at the dorsal parotid poles, sharp demarcation, also a small branch medially. **b** T1-weighted spin echo sequence, gadolinium DTPA, fat-suppressed lesion of the parotid gland with complete loss of signal after fat suppression (*arrows*), discrete constant edge enhancement, so such criteria are documented in a lipoma

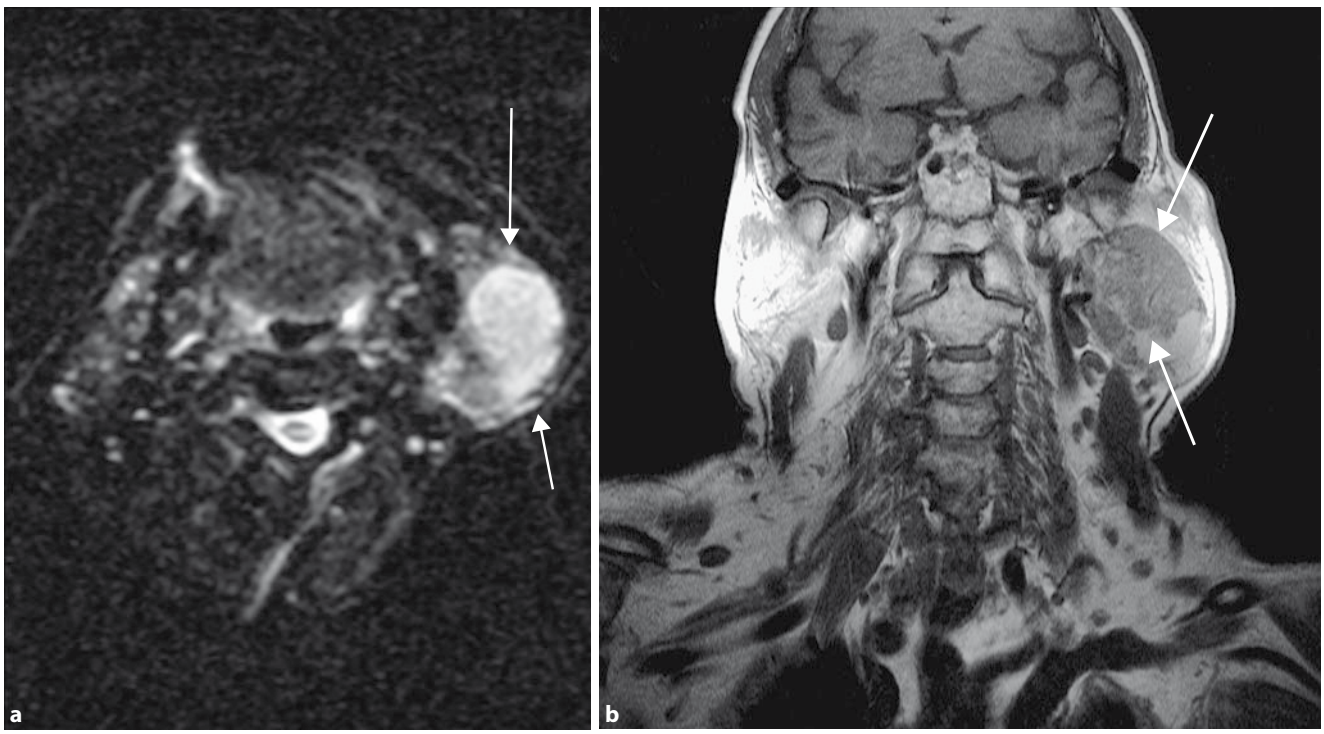

Fig. 16.9a,b Adenocarcinoma of the parotid gland (*arrows*)**. a** Diffusion-weighted MR sequence, TR/TE = 8,000 / 20. Increased signal intensity in the range of the mass on the left side of the parotid gland secured with adenocarcinoma histology, superficial as the lower lobe. The medial necrotic sections show low signal intensity. **b** Frontal T1-weighted MR sequence, TR/TE = 500 / 17, unenhanced. Frontally, swelling of the parotid gland is shown on the left side and a space-occupying lesion in the medial lobe with central liquid sections

16.6 Systemic Diseases

The systemic diseases include autoimmune diseases (HIV-associated changes in sarcoidosis and Sjögren's disease). On CT, individual granulated calcifications are documented. The MRI and MR sialography proved to be indicative of the assessment architecture of the glands.

Imaging. On MRI, a typical and pepper pattern with areas of increased and decreased signal intensity ion T1-weighted sequences.
The cysts thus appear hypointense. On T2-weighted sequences the areas of increased signal intensity appear partly cystic MR sialography allows the demarcation of the duct and the documentation of the location. The morphological diagnosis of Sjögren's disease is thus of great importance, because the early development of lymphoma and non-Hodgkin's lymphoma must be evaluated. These are often found in Sjögren's disease and appear as hypointense, confluent areas within the damaged gland architecture. Among the systemic diseases include autoimmune diseases (HIV-associated changes in sarcoidosis and Sjögren's disease) by CT, individually granulated calcifications are documented. MRI and MR sialography proved to be indicative of the assessment architecture of the glands.

16.7 Summary

In summary, basic imaging diagnostics of diseases the salivary glands evaluated primarily based on the clinical assessment and also imaging techniques, such as MRI and CT sialography and (Fig. 16.10).

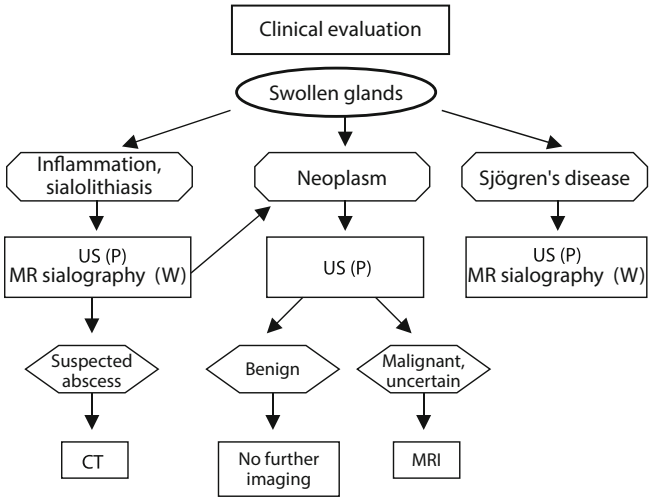

Fig. 16.10 Diagnostic flow chart for diseases of the salivary glands